New bi-dimensional SPAD arrays for Time Resolved Single Photon Imaging

R. Grasso[a,c], S. Tudisco[a], C. Piemonte[b], D. Lo Presti[a,c]
A. Anzalone[a], F. Musumeci[a,c], N. Randazzo[a], A. Scordino[a,c], N. Serra[b], N. Zorzi[b]

[a] *INFN – Laboratori Nazionali del Sud and Sez. INFN, Via S. Sofia 62, 95125, Catania, Italy*
[b] *FBK – Fondazione Bruno Kessler, Via S. Croce 77, 38122, Trento, Italy*
[c] *Dipartimento di Fisica e Astronomia, Catania University, Via S. Sofia 64, 95123, Catania, Italy*

Abstract

The studies in nuclear and plasma physics, astronomy, biomedicine, biophysics, and other fields require detectors able to perform the time resolved imaging of photons and charged particles. The Single Photon Avalanche Diodes (SPADs) arrays are devices able to acquire time resolved images with single photon sensitivity [1-7]. However the optimization and miniaturization of these photo-detectors is an open question. In this contribution we present the first electrical and optical characteristics of a new SPADs array architecture with passive quenching circuit. This solution allows to use a rows x columns readout strategy characterized by a number of reading channels of 2n instead of n^2.

The new SPAD architecture

The SPAD array is a nxn matrix of solid-state photo-detectors, i.e. diodes, electrically and optically insulated, working in Geiger mode. Its electrical and optical characteristics are strictly connected to the pixel active area and to the quenching resistor value (if passive quenching technique is used). [8-10]
We tested a new layout of SPAD array [11,12] with different active areas and quenching resistor values. The showed data refer to one of this prototype. In this new array architecture (see fig. 1), the pixels, arranged in a nxn regular square grid (n=18), were vertically crossed by n column buses and horizontally crossed by n row buses. Each diode cathode had two integrated quenching resistors, respectively connected to the row bus and to a column bus. The diode anodes were common.

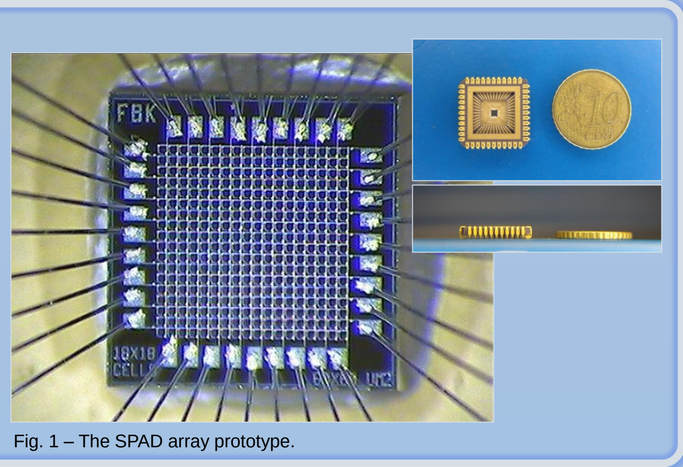

Fig. 1 – The SPAD array prototype.

Time Resolved Single Photon Imaging

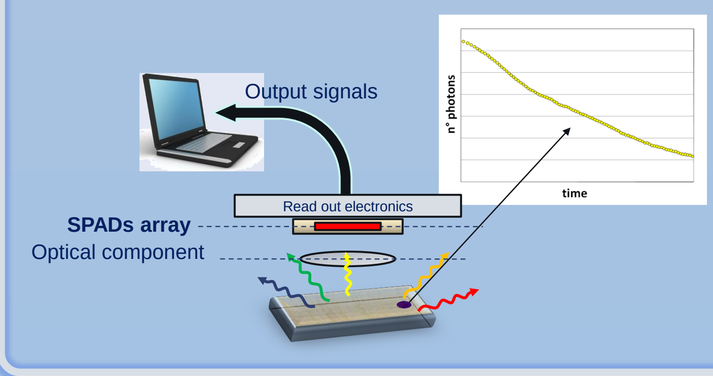

The static characteristics

The forward and reverse *current Vs. voltage* characteristics were measured between one of the output pads and the common anode.
The forward characteristic is reported in fig. 2. The output current grows linearly with forward-bias voltage due to the ohmic drop R_{on} that mask the exponential *i-V* characteristic. The R_{on} value can be deduced from the linear fit and the quenching resistor values R_q can be evaluated by observing that the output current is the sum of the *n* currents generated by the *n* diodes connected to the bus, that is $R_q = nR_{on}$. One assumes that the parasitic resistances are negligible compared to R_q value.
Figure 3 shows the reverse characteristic and the zoom of the reverse breakdown region. The reverse current start to became sufficiently high (in the order of few μA) when the reverse voltage is about 43.5V. The latter is so the expected breakdown voltage for this SPAD array.

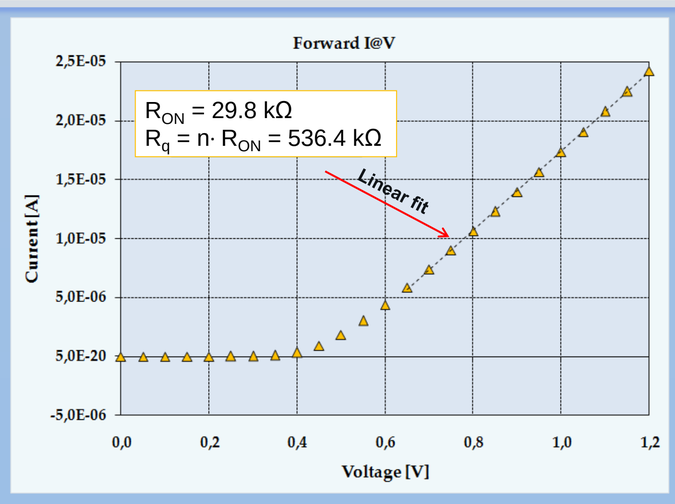

Fig. 2 – Typical forward current vs. voltage characteristic

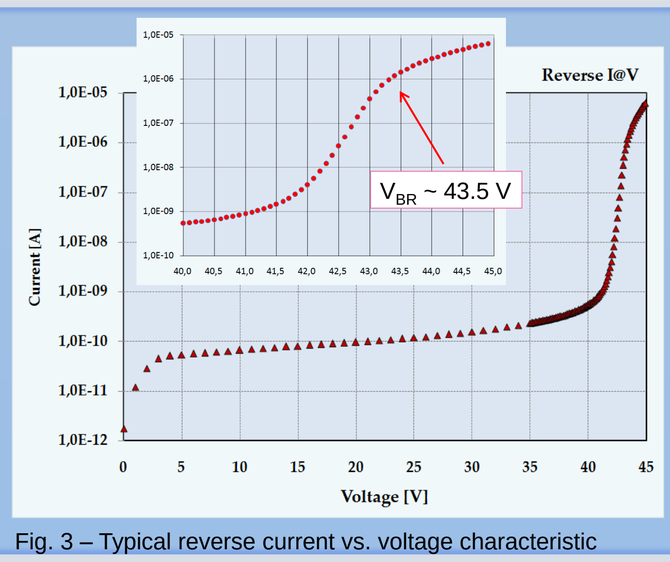

Fig. 3 – Typical reverse current vs. voltage characteristic

The dynamic characteristics

The showed dynamic characteristics were measured under single photon condition at room temperature. The SPAD arrays were biased using a power supply (HP 6234A) and lighted by a properly tuned Picosecond Injection Laser (Optical Head: PiL040, Control Unit: EIG1000D). The tested SPAD array outputs were directly connected to a four channels 1 GHz bandwidth digital oscilloscope (LeCroy WavePro 7100) and loaded with the 50 Ω oscilloscope input impedance.
Figure 4 shows a typical output signal observed at 15% overvoltage. The rise time and FWHM are respectively about 800 ps and 1 ns. This performance is obviously dependent on the quenching resistor and the active area values. The fluctuation observed in the falling edge is due to the coupling with cable and oscilloscope input impedance. The recharge time is about 100 – 150 ns (data not showed).
To evaluate the SPAD pixel gain and the output avalanche charge, the column bus and a row bus output pulses were acquired by two oscilloscope channels. These channels were triggered using logic Boolean AND operator. In this way the pixel was selected. The sum operator was applied to the collected signal pulses and the area of the sum signal was estimated. From these data the gain and the avalanche output charge were extrapolated and reported in fig. 5 as function of bias reverse voltage. The parameters of the data linear fit give information about the breakdown voltage (43.57V), and the pixel output capacitance (about 80 fF).

The timing resolution of a SPAD pixel was estimated collecting column bus and row bus output pulses triggered using logic Boolean AND operator, as we did in the case of gain and output charge evaluation. As reference signal to estimate the timing jitter, the laser trigger output was used. This trigger signal was acquired by one of the oscilloscope channels through its 50 Ω internal resistance. The delay between the reference signal and the bus output pulse, evaluated as the time between transition levels of the two sources, that is one of two signal pulses and trigger laser pulse, was histogrammed. Figure 6 shows an example of this histogram and of the corresponding Gaussian fit (R^2 = 0.98) when the SPAD array is biased at 10% overvoltage. Taking into account also the time jitter introduced by the oscilloscope and the laser source, the estimated FWHM is about 270 ps.

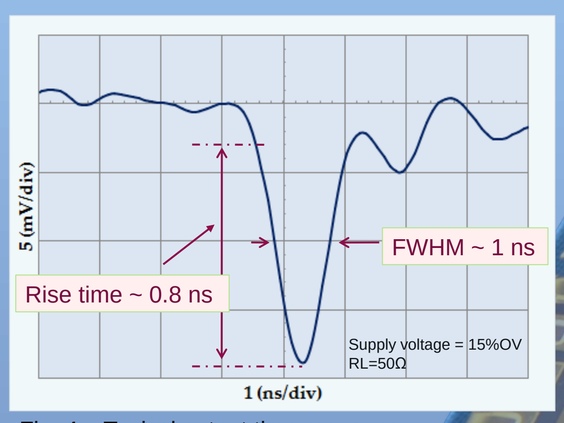

Fig. 4 – Typical output time response

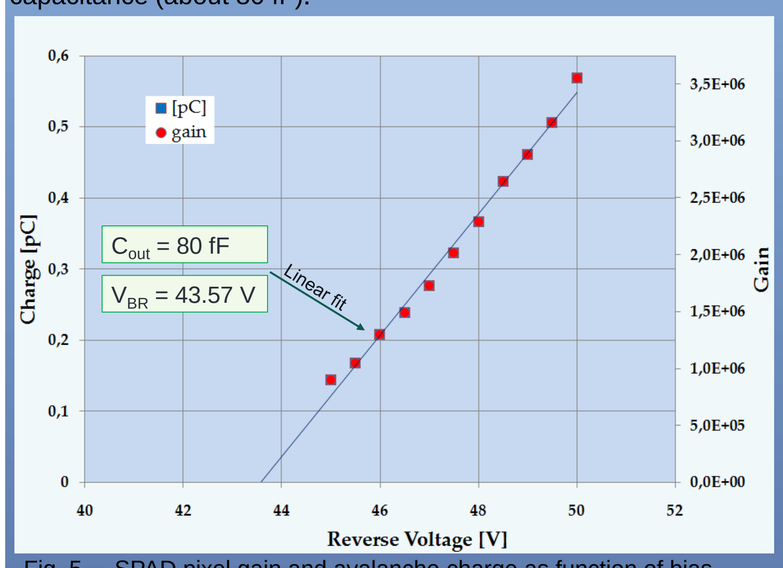

Fig. 5 – SPAD pixel gain and avalanche charge as function of bias reverse voltage

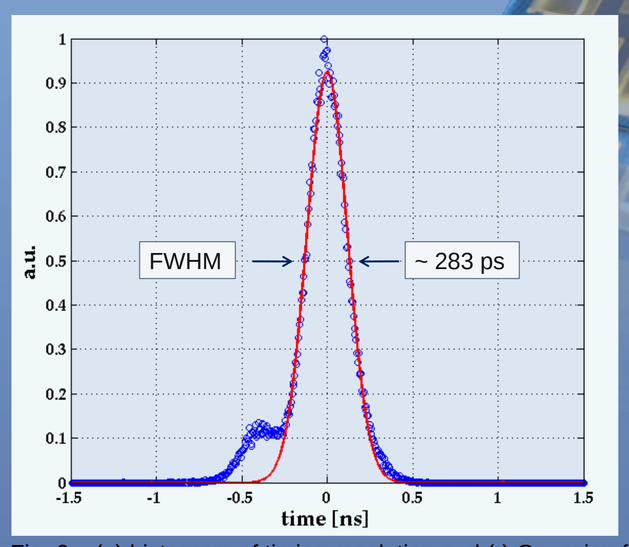

Fig. 6 – (o) histogram of timing resolution and (-) Gaussian fit

Conclusions

The data presented are obviously not exhaustive. However they show as the static and dynamic characteristics of this architecture are comparable with those of usual single SPADs. Moreover they prove that this architecture is good for time resolved image acquisitions. In fact the time performance and the timing resolution confirm the possibility to collect single photons with rate of tens of MHz and to discriminate the time of arrival of individual photon with an accuracy of hundreds of ps. The tests seem also to confirm an excellent ability to discriminate which pixel is turned on after the arrival of the photon.

[1] F. Musumeci et al., J. of Photchem. and Photobio. 79 (2005) 93.
[2] P. Finochiaro et al., J. of Mod. Optics 54 (1999) 199.
[3] S. Tudisco et al. Nucl. Phys. B Proc. Suppl. 150 (2006) 317
[4] D. Mascali et al., Rad. Eff. Def. in Solids 165 (2010) 730.
[5] S. Tudisco et al., NIMA 653 (2011) 47
[6] E. Sciacca et al. IEEE Phot. Tech. Lett. 18 (2006) 1633.
[7] M. Mazzillo et al., Sensors and Actuators 138 (2007) 306
[8] S. Privitera et al., Sensors 8 (2008) 4636
[9] S. Tudisco et al., Nuovo Cimento of Italian Phy. Soc. 30 (2007) 535.
[10] L. Neri et al., Sensors 10 (2010) 10828
[11] S. Tudiso et al., NIM A 610 (2009) 138.
[12] S.Tudisco, Advanced Photonic Sciences book, chap.12 pag. 303
Dr. Mohamed Fadhali (Ed.), Intch 2012